

# Synthesis of Stable Nanographenes with OBO-Doped Zigzag Edges Based on Tandem Demethylation-Electrophilic Borylation

Xiao-Ye Wang,<sup>†</sup> Akimitsu Narita,<sup>†</sup> Wen Zhang,<sup>†</sup> Xinliang Feng,<sup>\*,‡</sup> and Klaus Müllen<sup>\*,†</sup>

<sup>†</sup>Max Planck Institute for Polymer Research, Ackermannweg 10, 55128 Mainz, Germany

<sup>‡</sup>Center for Advancing Electronics Dresden and Department of Chemistry and Food Chemistry, Technische Universität Dresden, 01062 Dresden, Germany

**S** Supporting Information

**ABSTRACT:** A tandem demethylation-aryl borylation strategy was developed to synthesize OBO-doped tetrabenzo[*a,f,j,i,o*]perylene (namely “bistetracenes”) and tetrabenzo[*bc,ef,kl,no*]coronenes (namely “peritetracenes”). The OBO-doped bistetracene analogues exhibited excellent stability and strong fluorescence, in contrast to the unstable all-carbon bistetracene. Single-crystal X-ray analysis for OBO-doped bistetracene revealed a twisted double [5]helicene structure, indicating that this synthesis is applicable to new heterohelicenes. Importantly, cyclodehydrogenation of the bistetracene analogues successfully produced the unprecedented heteroatom-doped peritetracenes, which opened up a new avenue to periacene-type nanographenes with stable zigzag edges.

Acenes with linearly fused benzene rings have attracted tremendous attention during the past decades due to their promising physical properties and applications in organic electronics.<sup>1</sup> However, the instability of higher acenes toward oxidation and photodimerization severely limited further investigations.<sup>2</sup> Recently, several strategies, such as heteroatom doping and incorporation of five-membered rings, have been developed to access stable acene analogues,<sup>3</sup> which could be facilely handled.

Periacenes, two linear acenes laterally fused at all the *peri*-positions, are an important family of extended acene compounds.<sup>4</sup> The smaller members, perylene and bisanthene, have been known for a long time.<sup>5</sup> The longer homologues such as peritetracene (tetrabenzo[*bc,ef,kl,no*]coronene) and peripentacene (tetrabenzo[*bc,ef,mn,pq*]ovalene), which can be regarded as well-defined nanographenes with zigzag edges (Figure 1),<sup>6</sup> have remained elusive because of their high instability.<sup>7</sup> Only recently, in 2015, peripentacene was achieved on a metal surface under ultrahigh vacuum conditions by cyclodehydrogenation of a solution-synthesized precursor 6,6'-bipentacene.<sup>8</sup> On our way to periacenes, we have reported a bistetracene (1), namely tetrabenzo[*a,f,j,i,o*]perylene, in which two tetracenes are connected side by side with two single bonds.<sup>9</sup> Bistetracene exhibited distinct properties as compared with tetracene and could be viewed as a potential precursor of the unprecedented peritetracene. However, the bistetracene showed very poor stability and was quickly oxidized under ambient conditions, hindering detailed structural analyses and further cyclodehydrogenation toward peritetracene. Inspired by the strategy of

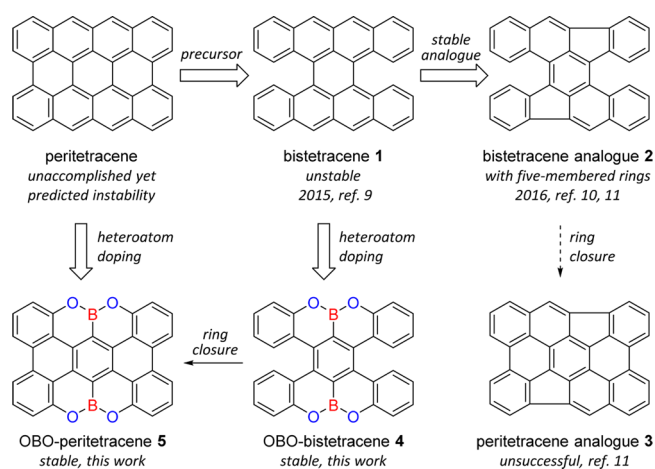


**Figure 1.** Chemical structures of peritetracene and its potential precursor bistetracene 1, a stable bistetracene analogue 2 with embedded five-membered rings, and its corresponding cyclodehydrogenated product 3, as well as OBO-doped bistetracene 4 and peritetracene 5 in this work. The substituents are omitted for simplicity.

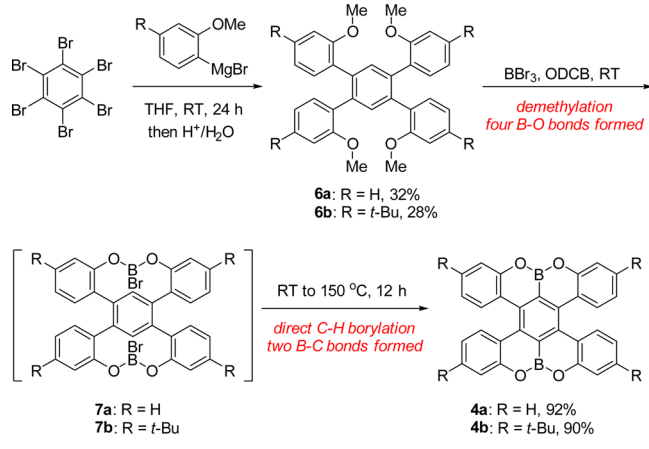
incorporating five-membered rings into acene systems to generate stable acene analogues, we described a bistetracene analogue with two five-membered rings, namely dibenzo[*a,m*]rubicene (2),<sup>10</sup> which was also synthesized by others through different approaches.<sup>11</sup> Bistetracene analogue 2 displayed excellent stability, which enabled full characterizations and applications in organic field-effect transistors.<sup>11</sup> These results suggested that targeting stable bisacene and periacene analogues is a promising way to develop novel materials by avoiding the instability issue. Nevertheless, cyclodehydrogenation of 2 failed to produce peritetracene analogue 3 with two embedded five-membered rings,<sup>11</sup> leaving the long pursued peritetracene framework still elusive.

Heteroatom-doped nanographenes are a promising class of molecules that possess different properties from their pristine hydrocarbon structures.<sup>12</sup> Especially, boron-doped nanographenes have received considerable interest in recent years, but the known examples are still limited due to the lack of efficient synthetic methods.<sup>13</sup> Herein, we developed tandem demethylation-borylation to synthesize an OBO-fused bistetracene analogue 4, which exhibited excellent stability and allowed

Received: April 21, 2016

Published: July 4, 2016

## Scheme 1. Synthetic Route to OBO-Doped Bistetracenes



comprehensive characterizations. Further cyclodehydrogenation of **4** successfully provided the first example of heteroatom-doped peritetracene (**5**) with OBO units on the edges, representing an important step forward toward stable zigzag-edged nanographenes.

The synthesis of compounds **4a** and **4b** is illustrated in Scheme 1. Treatment of hexabromobenzene with (2-methoxyphenyl)magnesium bromide in THF provided 1,2,4,5-tetra(2-methoxyphenyl)benzene (**6a**) after quenching the mixture with dilute hydrochloric acid.<sup>14</sup> Simply heating a solution of compound **6a** in *o*-dichlorobenzene (ODCB) at 150 °C in the presence of BBr<sub>3</sub> gave OBO-doped bistetracene **4a** in 92% yield. The reaction presumably included a demethylation process to form intermediate **7a** with four new B–O bonds, followed by electrophilic borylation on the central benzene to provide two extra C–B bonds. Compound **4b** with *tert*-butyl groups was synthesized in the same manner. During the preparation of this manuscript, Hatakeyama et al. independently reported the same compound **4a** and its derivative as double helicenes for the study of chiroptical properties.<sup>15</sup> Compared to Hatakeyama's method where lithium-halogen exchange on the central benzene was first performed to introduce boron, followed by cyclization with oxygen to give the OBO-fused compounds in 55–60% yields, the method presented here is overall simpler, involving direct C–H borylation, and more efficient with higher yields. Compounds **4a** and **4b** were stable enough to be purified by column chromatography over silica gel and recrystallization from CH<sub>2</sub>Cl<sub>2</sub>/MeOH. No obvious decomposition was observed during this process. The solids are stable even after storing under ambient conditions for more than six months, showing no detectable change in <sup>1</sup>H NMR spectra.

The single crystal of compound **4a** was successfully grown from CHCl<sub>3</sub>/EtOH, so that its structure was unambiguously determined by single-crystal X-ray analysis. As depicted in Figure 2a, the B–C bond length is around 1.52 Å, indicating a single bond character. The B–O bond length is around 1.37 Å, a typical value for three-coordinated boron–oxygen compounds.<sup>16</sup> The molecule adopts a twisted conformation. The dihedral angles for C1–C2–C3–C4 and C5–C6–C7–C8 are 32.3° and 28.2°, respectively. The central benzene ring exhibits one of the highest distortions reported in the literature,<sup>17</sup> with a torsion angle of 24.5° for C9–C2–C3–C10 (also defined by the three blue bonds in Figure 2a). The twisted bistetracene analogue **4a** is actually a double hetero[5]helicene<sup>18</sup> with a pair of enantiomers in one unit cell (Figure 2b). Hatakeyama et al. have successfully

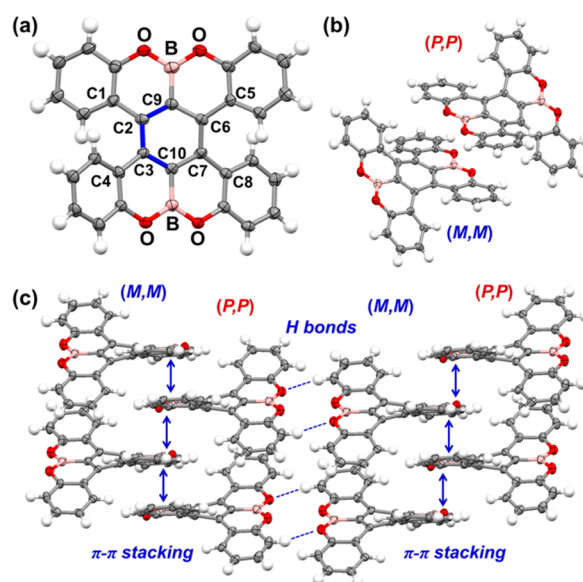


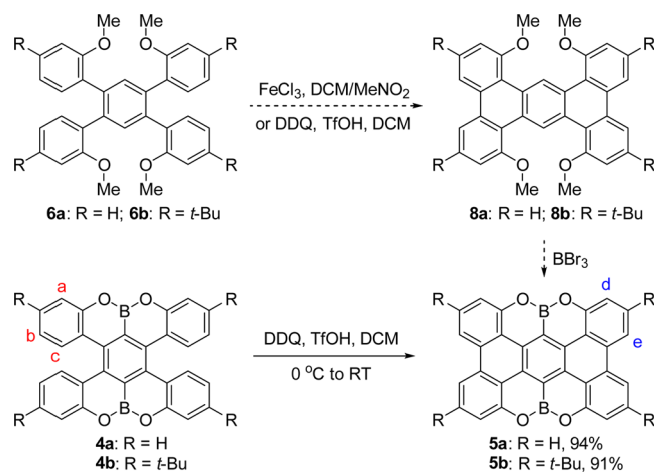
Figure 2. Single-crystal structure of **4a** with thermal ellipsoids shown at 50% probability. (a) Top view. (b) A pair of enantiomers in one unit cell. (c) Crystal packing structure.

separated the chiral isomers by increasing the isomerization barrier through the introduction of *tert*-butyl groups at the *para*-positions with respect to the oxygen.<sup>15</sup> In our racemic crystal of **4a**, the (*P,P*)- and (*M,M*)-isomers are packed in an alternating fashion, forming close  $\pi$ -stacking structures (interlayer distance: 3.2–3.4 Å) with multiple O···H hydrogen bonds (Figure 2c).

To further understand the distorted conformation of compound **4a**, DFT calculations were performed to investigate the properties of the experimentally missing *meso*-isomer (*P,M*)-**4a**. According to the optimizations at the B3LYP/6-311G(d,p) level, (*P,M*)-**4a**, which adopts an *anti*-folded conformation, is 24.1 kJ/mol higher in energy than the twisted (*P,P*)- or (*M,M*)-isomers (Figure S2). The large energy difference indicates that the twisted conformations are thermodynamically more stable, in agreement with the experimental observation.

With the ultimate goal of accessing OBO-doped peritetracene, we first tried the cyclodehydrogenation of compounds **6a** and **6b** with FeCl<sub>3</sub> or DDQ/TfOH (Scheme 2). These conditions failed to give the expected products **8a** and **8b**. Nevertheless, the

## Scheme 2. Synthesis of OBO-Doped Peritetracenes



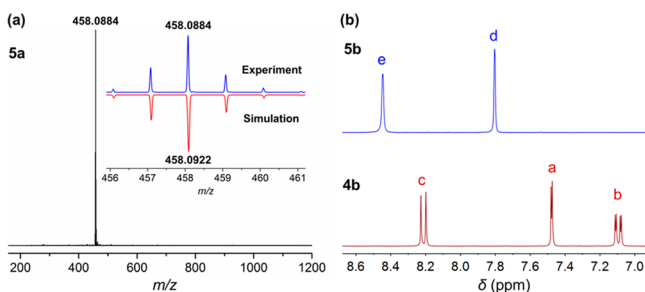


**Figure 3.** (a) High-resolution MALDI-TOF MS spectrum of OBO-doped peritetracene **5a**. Inset: the corresponding experimental and simulated isotopic distributions. (b) Aromatic regions of the  $^1\text{H}$  NMR spectra of **4b** and **5b**.

cyclodehydrogenation of **4a** and **4b** in the presence of DDQ/TfOH cleanly turned the twisted bistetracene analogues into the planar nanographene molecules **5a** and **5b** in excellent yields (91–94%). This result at the same time indicated the high stability of the OBO-peritetracenes under the acidic and oxidative conditions. The structure of **5a** was confirmed by high-resolution mass spectrometry (HRMS), which showed a single peak at  $m/z = 458.0884$  Da, in good agreement with its expected molecular mass of 458.0922 Da (Figure 3a). The isotopic distribution observed for **5a** also perfectly matched with the simulated pattern, corroborating the successful cyclodehydrogenation. However, the poor solubility of **5a** prevented further characterizations. The introduction of *t*-Bu groups substantially increased the solubility of the nanographene molecule in common organic solvents. A well-resolved  $^1\text{H}$  NMR spectrum of **5b** could be recorded in  $\text{C}_2\text{D}_2\text{Cl}_4$  (Figure 3b, for full spectra, see the Supporting Information). Compared to the spectrum of **4b** with three sets of aromatic proton signals, two singlets were observed for **5b**, clearly demonstrating its chemical structure. Different from the unstable all-carbon peritetracene, the OBO-doped analogues **5a** and **5b** displayed excellent stability under ambient conditions, facilitating all further characterizations.

The photophysical properties of **4a**, **4b**, and **5b** were investigated in  $\text{CH}_2\text{Cl}_2$  solutions (Figure 4). The optical gaps of **4a** and **4b** deduced from the absorption onsets are 2.88 and 2.83 eV, respectively, which are larger than that of the carbon analogue bistetracene **1**.<sup>9</sup> Different from the nonfluorescent bistetracene **1**, compounds **4a** and **4b** both exhibited strong fluorescence with high quantum yields of 61% and 52%, respectively. When the twisted **4b** was planarized into OBO-peritetracene **5b**, well-resolved vibronic structures were observed for both the absorption and fluorescence spectra. A blue fluorescence with a quantum yield of 27% was recorded, with the spectrum displaying almost the mirror image of the low-energy absorption band. The Stokes shift was as small as 7 nm, indicating the rigid structure of this nanographene molecule.

The electrochemical properties of the OBO-fused compounds were studied by cyclic voltammetry (Figure S1). With ferrocene as an external standard, the HOMO and LUMO energy levels of **4a** were estimated to be  $-5.86$  and  $-2.96$  eV, respectively. The *t*-Bu groups on **4b** significantly raised the HOMO to  $-5.54$  eV and the LUMO to  $-2.72$  eV. The electrochemical HOMO–LUMO gaps of **4a** and **4b** are thus 2.90 and 2.82 eV, respectively, which are in good agreement with the optical gaps (Table S1). Only the oxidative wave was observed for **5b**, whose HOMO was determined as  $-5.87$  eV. The LUMO level of **5b** was calculated to be  $-3.03$  eV based on the HOMO level and the optical gap.

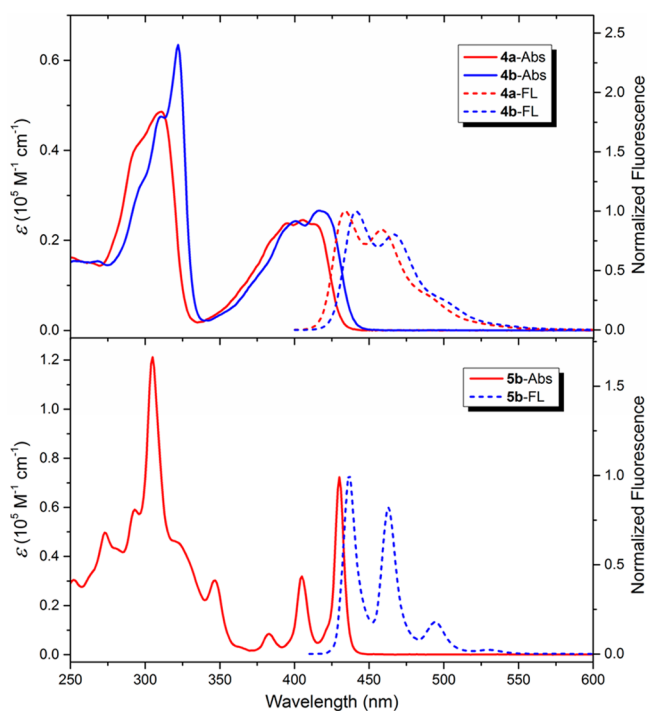


**Figure 4.** Absorption and fluorescence spectra (excited at the absorption maxima) of compounds **4a**, **4b**, and **5b** in  $\text{CH}_2\text{Cl}_2$  ( $1 \times 10^{-5}$  M).

For gaining deeper insight into the effect of heteroatom incorporation, DFT calculations were performed to compare the electronic properties of pristine peritetracene and the OBO-doped analogue (Figure 5). According to the NICS calculations,

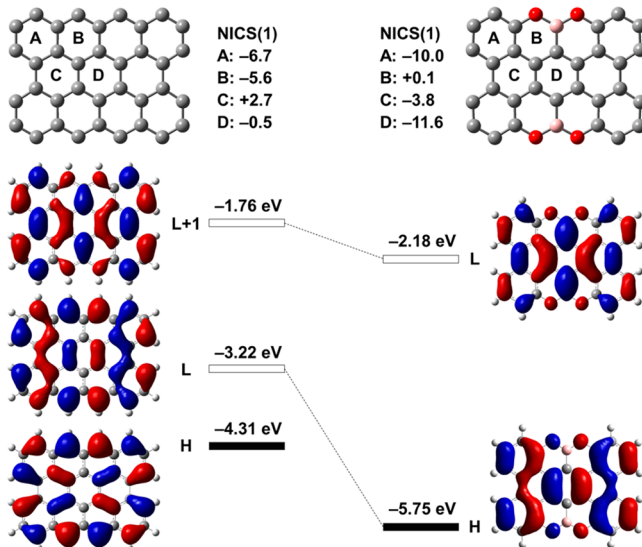


**Figure 5.** DFT-calculated NICS(1) values (in ppm), molecular orbitals, and energy diagrams of peritetracene (left) and OBO-doped peritetracene (right). The orbitals connected by the dashed lines exhibit similar distributions. H: HOMO; L: LUMO.

the benzene rings A and B in peritetracene display moderate aromaticity, whereas C and D rings are weakly antiaromatic and nonaromatic, respectively. Differently, A and D rings in OBO-doped peritetracene are highly aromatic, whereas ring B is nonaromatic and ring C exhibits low aromaticity. These results indicated that the heteroatoms significantly modified the



electronic structures of the carbon framework. A closer look into the molecular orbitals of both molecules suggested that the HOMO and LUMO distributions of OBO-doped peritetracene are very similar to the LUMO and LUMO+1 distributions of peritetracene, respectively. Considering the different valence electrons of CCC (3  $p_z$  electrons) and OBO (4  $p_z$  electrons) units, OBO-doped peritetracene should possess two more  $p_z$  electrons, which are filled in the orbital corresponding to the LUMO of peritetracene to give the HOMO of OBO-doped peritetracene. Importantly, the heteroatom doping results in a low-lying HOMO, which contributes to the high stability of OBO-peritetracenes. Furthermore, comparison of the electronic structures of OBO-doped peritetracene and those of tetrabenzoanthracene derivatives with and without alkyl substituents indicates that the OBO unit cannot be simply viewed as a structural linkage, but has a significant impact on the electronic properties (Figure S7).

In summary, we have developed a tandem demethylation-electrophilic borylation method to synthesize new OBO-doped bistetracenes, which exhibit good stability and strong fluorescence as compared to the ambient sensitive, nonfluorescent bistetracene **1**. Single-crystal X-ray analysis revealed a double hetero[5]helicene structure with a highly twisted benzene ring. Cyclodehydrogenation successfully generated the first example of heteroatom-doped peritetracenes, which opened a new strategy to stabilize zigzag edges of periacenes. This work offers new possibilities not only for the synthesis of twisted double helicenes but also for the construction of planar zigzag-edged nanographenes, in particular higher periacenes and eventually zigzag-edged graphene nanoribbons, with excellent stability.

## ■ ASSOCIATED CONTENT

### Supporting Information

The Supporting Information is available free of charge on the ACS Publications website at DOI: 10.1021/jacs.6b04092.

Experimental details and data (PDF)

Crystallographic data for **4a** (CIF)

## ■ AUTHOR INFORMATION

### Corresponding Authors

\*xinliang.feng@tu-dresden.de

\*muellen@mpip-mainz.mpg.de

### Notes

The authors declare no competing financial interest.

## ■ ACKNOWLEDGMENTS

The authors sincerely thank Dr. Dieter Schollmeyer (Institute for Organic Chemistry, Johannes Gutenberg University Mainz) for single-crystal X-ray structural analysis. X.-Y.W. is grateful for the fellowship from Alexander von Humboldt Foundation. We acknowledge the financial support from DFG Priority Program SPP 1459, Graphene Flagship (CNECT-ICT-604391), and European Union Project MoQuaS.

## ■ REFERENCES

- (1) (a) Bendikov, M.; Wudl, F.; Perepichka, D. F. *Chem. Rev.* **2004**, *104*, 4891. (b) Anthony, J. E. *Chem. Rev.* **2006**, *106*, 5028. (c) Anthony, J. E. *Angew. Chem., Int. Ed.* **2008**, *47*, 452. (d) Ye, Q.; Chi, C. *Chem. Mater.* **2014**, *26*, 4046.
- (2) (a) Chan, S. H.; Lee, H. K.; Wang, Y. M.; Fu, N. Y.; Chen, X. M.; Cai, Z. W.; Wong, H. N. C. *Chem. Commun.* **2005**, 66. (b) Bénard, C. P.; Geng, Z.; Heuft, M. A.; VanCrey, K.; Fallis, A. G. *J. Org. Chem.* **2007**, *72*,

7229. (c) Kaur, I.; Jia, W.; Kopeski, R. P.; Selvarasah, S.; Dokmeci, M. R.; Pramanik, C.; McGruer, N. E.; Miller, G. P. *J. Am. Chem. Soc.* **2008**, *130*, 16274. (d) Purushothaman, B.; Parkin, S. R.; Anthony, J. E. *Org. Lett.* **2010**, *12*, 2060. (e) Zade, S. S.; Bendikov, M. *Angew. Chem., Int. Ed.* **2010**, *49*, 4012. (f) Tönshoff, C.; Bettinger, H. F. *Angew. Chem., Int. Ed.* **2010**, *49*, 4125. (g) Purushothaman, B.; Bruzek, M.; Parkin, S. R.; Miller, A.-F.; Anthony, J. E. *Angew. Chem., Int. Ed.* **2011**, *50*, 7013. (h) Bettinger, H. F.; Tönshoff, C. *Chem. Rec.* **2015**, *15*, 364.

- (3) (a) Bunz, U. H. F. *Acc. Chem. Res.* **2015**, *48*, 1676. (b) Bunz, U. H. F.; Engelhart, J. U.; Lindner, B. D.; Schaffroth, M. *Angew. Chem., Int. Ed.* **2013**, *52*, 3810. (c) Endres, A. H.; Schaffroth, M.; Paulus, F.; Reiss, H.; Wadeh, H.; Rominger, F.; Krämer, R.; Bunz, U. H. F. *J. Am. Chem. Soc.* **2016**, *138*, 1792. (d) Takimiya, K.; Osaka, I.; Mori, T.; Nakano, M. *Acc. Chem. Res.* **2014**, *47*, 1493. (e) Dai, G.; Chang, J.; Luo, J.; Dong, S.; Aratani, N.; Zheng, B.; Huang, K.-W.; Yamada, H.; Chi, C. *Angew. Chem., Int. Ed.* **2016**, *55*, 2693. (f) Shi, X.; Kueh, W.; Zheng, B.; Huang, K.-W.; Chi, C. *Angew. Chem., Int. Ed.* **2015**, *54*, 14412. (g) Chase, D. T.; Fix, A. G.; Kang, S. J.; Rose, B. D.; Weber, C. D.; Zhong, Y.; Zakharov, L. N.; Lonergan, M. C.; Nuckolls, C.; Haley, M. M. *J. Am. Chem. Soc.* **2012**, *134*, 10349. (h) Neue, B.; Araneda, J. F.; Piers, W. E.; Parvez, M. *Angew. Chem., Int. Ed.* **2013**, *52*, 9966.

- (4) Sun, Z.; Ye, Q.; Chi, C.; Wu, J. *Chem. Soc. Rev.* **2012**, *41*, 7857.
- (5) (a) Fort, E. H.; Donovan, P. M.; Scott, L. T. *J. Am. Chem. Soc.* **2009**, *131*, 16006. (b) Fort, E. H.; Scott, L. T. *Angew. Chem., Int. Ed.* **2010**, *49*, 6626. (c) Li, J.; Zhang, K.; Zhang, X.; Huang, K.-W.; Chi, C.; Wu, J. *J. Org. Chem.* **2010**, *75*, 856.
- (6) (a) Matsumoto, A.; Suzuki, M.; Kuzuhara, D.; Hayashi, H.; Aratani, N.; Yamada, H. *Angew. Chem., Int. Ed.* **2015**, *54*, 8175. (b) Dorel, R.; Manzano, C.; Grisolia, M.; Soe, W.-H.; Joachim, C.; Echavarren, A. M. *Chem. Commun.* **2015**, 51, 6932. (c) Zöphel, L.; Berger, R.; Gao, P.; Enkelmann, V.; Baumgarten, M.; Wagner, M.; Müllen, K. *Chem. - Eur. J.* **2013**, *19*, 17821.
- (7) (a) Northrop, B. H.; Norton, J. E.; Houk, K. N. *J. Am. Chem. Soc.* **2007**, *129*, 6536. (b) Jiang, D.-E.; Dai, S. *Chem. Phys. Lett.* **2008**, *466*, 72. (c) Roberson, L. B.; Kowalik, J.; Tolbert, L. M.; Kloc, C.; Zeis, R.; Chi, X.; Fleming, R.; Wilkins, C. J. *J. Am. Chem. Soc.* **2005**, *127*, 3069.
- (8) Rogers, C.; Chen, C.; Pedramrazi, Z.; Omrani, A. A.; Tsai, H.-Z.; Jung, H. S.; Lin, S.; Crommie, M. F.; Fischer, F. R. *Angew. Chem., Int. Ed.* **2015**, *54*, 15143.
- (9) Liu, J.; Ravat, P.; Wagner, M.; Baumgarten, M.; Feng, X.; Müllen, K. *Angew. Chem., Int. Ed.* **2015**, *54*, 12442.
- (10) Liu, J.; Narita, A.; Osella, S.; Zhang, W.; Schollmeyer, D.; Beljonne, D.; Feng, X.; Müllen, K. *J. Am. Chem. Soc.* **2016**, *138*, 2602.
- (11) Gu, X.; Xu, X.; Li, H.; Liu, Z.; Miao, Q. *J. Am. Chem. Soc.* **2015**, *137*, 16203.
- (12) Narita, A.; Wang, X.-Y.; Feng, X.; Müllen, K. *Chem. Soc. Rev.* **2015**, *44*, 6616.
- (13) (a) Wang, X.-Y.; Zhuang, F.-D.; Wang, R.-B.; Wang, X.-C.; Cao, X.-Y.; Wang, J.-Y.; Pei, J. *J. Am. Chem. Soc.* **2014**, *136*, 3764. (b) Kriegl, M.; Reicherter, F.; Haiss, P.; Ströbele, M.; Eichele, K.; Treanor, M.-J.; Schaub, R.; Bettinger, H. F. *Angew. Chem., Int. Ed.* **2015**, *54*, 8284. (c) Hertz, V. M.; Bolte, M.; Lerner, H.-W.; Wagner, M. *Angew. Chem., Int. Ed.* **2015**, *54*, 8800. (d) Dou, C.; Saito, S.; Matsuo, K.; Hisaki, I.; Yamaguchi, S. *Angew. Chem., Int. Ed.* **2012**, *51*, 12206. (e) Wang, X.-Y.; Wang, J.-Y.; Pei, J. *Chem. - Eur. J.* **2015**, *21*, 3528. (f) Escande, A.; Ingleson, M. J. *Chem. Commun.* **2015**, 51, 6257.
- (14) (a) Yang, X.; Dou, X.; Müllen, K. *Chem. - Asian J.* **2008**, *3*, 759. (b) Harada, K.; Hart, H.; Frank Du, C. J. *J. Org. Chem.* **1985**, *50*, 5524.
- (15) Katayama, T.; Nakatsuka, S.; Hirai, H.; Yasuda, N.; Kumar, J.; Kawai, T.; Hatakeyama, T. *J. Am. Chem. Soc.* **2016**, *138*, 5210.
- (16) Coulson, C. A.; Dingle, T. W. *Acta Crystallogr., Sect. B: Struct. Crystallogr. Cryst. Chem.* **1968**, *24*, 153.
- (17) (a) Lu, J.; Ho, D. M.; Vogelaar, N. J.; Kraml, C. M.; Pascal, R. A. *J. Am. Chem. Soc.* **2004**, *126*, 11168. (b) Hashimoto, S.; Nakatsuka, S.; Nakamura, M.; Hatakeyama, T. *Angew. Chem., Int. Ed.* **2014**, *53*, 14074.
- (18) (a) Fujikawa, T.; Segawa, Y.; Itami, K. *J. Am. Chem. Soc.* **2015**, *137*, 7763. (b) Sakamaki, D.; Kumano, D.; Yashima, E.; Seki, S. *Angew. Chem., Int. Ed.* **2015**, *54*, 5404.